

# Search for single production of the heavy vectorlike $T$ quark with $T \rightarrow th$ and $h \rightarrow \gamma\gamma$ at the high-luminosity LHC

Yao-Bei Liu\*

*Henan Institute of Science and Technology, Xinxiang 453003, People's Republic of China*

(Received 22 October 2016; published 10 February 2017)

The vectorlike top partners  $T$  are predicted in many extensions of the Standard Model (SM). In a simplified model including a single vectorlike  $T$  quark with charge 2/3, we investigate the process  $pp \rightarrow Tj$  induced by the couplings between the top partner with the first and the third generation quarks at the LHC. We find that the mixing with the first generation can enhance the production cross section. We further study the observability of the single heavy top partner through the process  $pp \rightarrow T(\rightarrow th)j \rightarrow t(\rightarrow b\ell\nu_\ell)h(\rightarrow \gamma\gamma)j$  at the high-luminosity (HL)-LHC (a 14 TeV  $pp$  collider with an integrated luminosity of  $3 \text{ ab}^{-1}$ ). For three typical heavy  $T$  quark masses  $m_T = 600, 800$  and  $1000 \text{ GeV}$ , the  $3\sigma$  exclusion limits, as well as the  $5\sigma$  discovery reach in the parameter plane of the two variables  $g^* - R_L$ , are respectively obtained at the HL-LHC.

DOI: 10.1103/PhysRevD.95.035013

## I. INTRODUCTION

The discovery of a 125 GeV Higgs boson at the CERN LHC [1,2] has heralded the beginning of a new era of Higgs physics. However, it is theoretically difficult to understand why the Higgs boson has a mass of  $\sim 100 \text{ GeV}$ . In order to offer a potential solution to the hierarchy problem, many new physics theories beyond the Standard Model (SM) predict the existence of new heavy fermions, which can stabilize the Higgs boson mass and protect it from dangerous quadratic divergences [3,4]. In many cases, such as little Higgs models [5], extra dimensions (ED) [6], composite Higgs models [7], and twin Higgs models [8], etc. these new heavy fermions are heavy vectorlike top partners, which have the same spin and only differ in the embedding into representations of the weak isospin,  $SU(2)_L$ . The phenomenology of new heavy quarks has been widely studied in the literature; see for example [9–19].

Very recently, the ATLAS and CMS Collaborations have performed the searches for  $T$  quarks and have placed limits on its mass ranging from 720 to 950 GeV for different  $T$  quark branching fractions ( $bW$ ,  $tZ$  and  $th$ ) [20,21]. Most of these experimental searches assume the  $T$  quarks to be pair produced via the strong interaction, and these bounds strongly depend on the assumptions on the decay branching ratios and the properties of the top partner. Apart from direct searches, the indirect searches for the top partners through their contributions to the electroweak precision observables [22,23], Z-pole observables [24,25] and the Higgs decay channels in the various final states [26–28] have been extensively investigated. As pointed out in Refs. [29–33], single production of top partners starts to dominate over pair production for high  $M_T$  (about

$M_T \gtrsim 1 \text{ TeV}$ ) due to larger phase space. Very recently, the analyses of the singly produced top partners that decay to  $bW$  and  $tZ$  have been performed in Refs. [34,35]. Furthermore, the authors in Ref. [36] studied the search strategies of the single top partner production with all the possible decay modes ( $tZ$ ,  $th$  and  $Wb$ ) by using the boosted object tagging methods. As a result, several ATLAS and CMS vectorlike quark searches also target their single production mode [37,38]. However, most of the studies are based on the assumption that the  $T$  quarks only couple to the first generation of quarks or the third generation  $b$  quark.

Considering the constraints from flavor physics [39–44], the top partners can mix in a sizable way with lighter quarks, which could have a severe impact on electroweak vectorlike quark processes at the LHC [45]. Using the cut-and-count analysis, the authors in Ref. [46] studied the LHC discovery potential of the  $T \rightarrow tZ$  channel in the trilepton decay mode in single production, for a singlet  $T$  quark mixing with the first generation. Such mixing can enhance the single production due to the presence of valence quarks in the initial state. In this work, we study the single vectorlike  $T$  quark production through the process  $pp \rightarrow T(\rightarrow th)j \rightarrow t(\rightarrow b\ell\nu_\ell)h(\rightarrow \gamma\gamma)j$  in a simplified model, as presented in Ref. [42]. The benefit of using the simplified effective theory is that the results of the studies could be used to make predictions for more complex models including various types of top partners (see, e.g., Refs. [46–51]). In comparison with the existing searches for other decay modes, the  $h \rightarrow \gamma\gamma$  channel has a small cross section but has the great advantage that most QCD backgrounds are gone, such as done in Refs. [52,53]. This has recently been done by the CMS Collaboration in events with at least one top partner undergoing the  $T \rightarrow th(h \rightarrow \gamma\gamma)$  decay chain from the  $T\bar{T}$  production [54],

\*liuyaobei@sina.com

which has excluded the existence of top quark partners with mass up to 540 GeV using  $19.7 \text{ fb}^{-1}$  of integrated luminosity under the hypothesis that  $\text{Br}(T \rightarrow th) = 100\%$ . The rough estimation in Ref. [36] has shown that it is challenging to observe the  $T$  quark with an  $h_{\gamma\gamma}$  signal at the 14 TeV with  $100 \text{ fb}^{-1}$  due to the small production cross section. Thus, here we consider the potential for the HL-LHC with an integrated luminosity of  $3 \text{ ab}^{-1}$ . We expect that such a channel may become complementary to other channels in the searches for the heavy vectorlike top partner.

This paper is arranged as follows. In Sec. II, we briefly describe the simplified model and calculate the single top partner production cross section involving the mixing with both the first and third generation quarks. In Sec. III, we discuss the observability of the top partner through the process  $pp \rightarrow T(\rightarrow th)j \rightarrow t(\rightarrow b\ell\nu_\ell)h(\rightarrow \gamma\gamma)j$  at the HL-LHC. Finally, a short summary is given in Sec. IV.

## II. TOP PARTNER IN THE SIMPLIFIED MODEL

### A. Brief review of the simplified model

To capture all the essential features of the new heavy top partners while remaining as model independent as possible, the authors of Ref. [42] have proposed a generic parametrization of an effective Lagrangian for top partners with different electromagnetic charge, where they considered vectorlike quarks embedded in general representations of the weak  $SU(2)$  group. Here we mainly consider the case in which the top partner is an  $SU(2)$  singlet and can mix and decay directly into the first and third generation quarks. The interactions of the vectorlike  $T$  quark with gluons and photons are governed by the gauge symmetries.

The simple Lagrangian that parametrizes the  $T$  couplings to quarks and electroweak bosons is [42]

$$\mathcal{L}_T = \frac{gg^*}{2} \left\{ \frac{S_R}{\sqrt{2}} [\bar{T}_L W_\mu^+ \gamma^\mu d_L] + \frac{C_R}{\sqrt{2}} [\bar{T}_L W_\mu^+ \gamma^\mu b_L] \right. \\ + \frac{S_R}{2 \cos \theta_W} [\bar{T}_L Z_\mu^+ \gamma^\mu u_L] + \frac{C_R}{2 \cos \theta_W} [\bar{T}_L Z_\mu^+ \gamma^\mu t_L] \\ - S_R \frac{M_T}{v} [\bar{T}_R h u_L] - C_R \frac{M_T}{v} [\bar{T}_R h t_L] - C_R \frac{m_t}{v} [\bar{T}_L h t_R] \Big\} \\ + \text{H.c.}, \quad (1)$$

where

$$S_R = \sqrt{\frac{R_L}{1 + R_L}}, \quad C_R = \sqrt{\frac{1}{1 + R_L}}. \quad (2)$$

In Eq. (1),  $g$  is the  $SU(2)_L$  gauge coupling constant,  $\theta_W$  is the Weinberg angle,  $v \approx 246$  GeV, and the subscripts  $L$  and  $R$  label the chiralities of the fermions. Besides the top partner mass  $m_T$ , there are two free parameters:

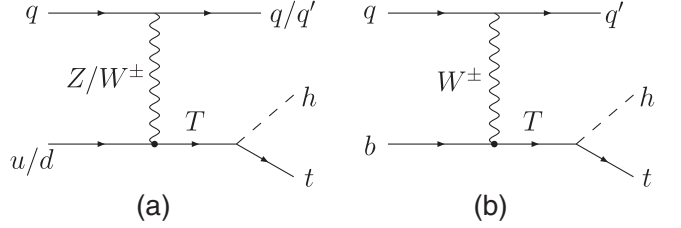


FIG. 1. Feynman diagrams for the process  $pp \rightarrow Tj \rightarrow thj$  at the LHC via couplings of the  $T$  to (a) first generation quarks and (b) third generation quarks.

- (i)  $g^*$ , the coupling strength to SM quarks in units of standard couplings, which is only relevant in single production. In general, the value of  $g^*$  can be taken in the range 0.1–0.5 [35]. A more complete description of the limits on the mixing with the vectorlike quarks has been studied in Ref. [25].
- (ii)  $R_L$ , the generation mixing coupling, which controls the share of the  $T$  coupling between first and third generation quarks. In the extreme case,  $R_L = 0$  and  $R_L = \infty$ , respectively, correspond to coupling to third generation quarks and first generation of quarks only.

For  $R_L = 0$ , the branching fractions of  $T$  into  $th$ ,  $tZ$  and  $bW$  reach a good approximation,<sup>1</sup> given by the ratios 1:1:2 as expected by the Goldstone boson equivalence theorem for a heavy singlet top partner [29]. It should be mentioned that not only can the nonvanishing  $R_L$  alter the branching ratios, but it can also alter the case when  $g^*$  gets close to 1 (see, e.g., Ref. [25]). A full study of the precision bounds of this particular model is beyond the scope of this paper, as we only use this model as illustration for top partner search strategies. As shown in Refs [39–45], these parameters can be constrained by the flavor physics and the oblique parameters. Here we take a conservative range for the mixing parameter:  $0 \leq R_L \leq 2$ . For some details about this effective Lagrangian in terms of complete models, one can see Refs. [35,42–44].

### B. Single production of top partner $T$

At the LHC, the top partner can be singly produced in association with a light jet. In this paper we mainly study the LHC discovery potential of the  $T$  quark from the decay channel  $T \rightarrow th$ . The Feynman diagrams for the process  $pp \rightarrow Tj \rightarrow thj$  are plotted in Fig. 1, where the top partner is produced due to the interaction with light quarks or due to the interaction with the  $b$  quark. From the Lagrangian in Eq. (1), we know that the production cross sections coming from these two sets of diagrams are very sensitive to the mixing coupling parameter  $R_L$ .

<sup>1</sup>Here we consider the case in which  $m_T \gg m_t$ , as shown in Ref. [35].

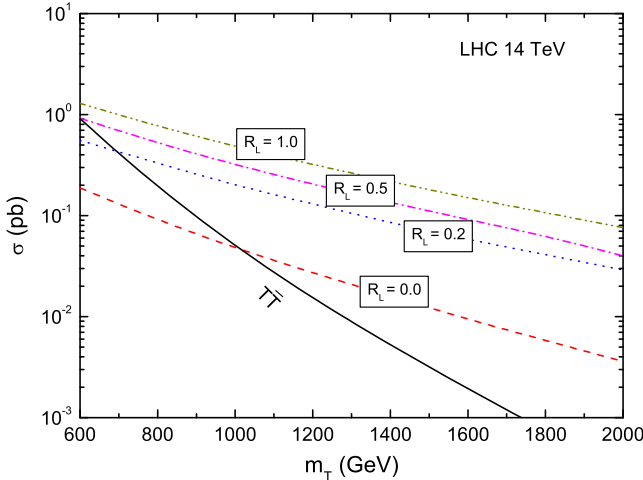


FIG. 2. The dependence of the cross sections  $\sigma$  for the process  $pp \rightarrow Tj + \bar{T}j$  on the  $T$  quark mass  $m_T$  at the 14 TeV LHC with  $g^* = 0.1$  and several values of  $R_L$ . The solid curves show the  $T\bar{T}$  pair production cross section.

The model file of the singlet  $T$  quark [55] is implemented via the FeynRules package [56]. The cross sections are calculated at tree level using MadGraph5-aMC@NLO [57] and checked by CalcHEP [58]. We use CTEQ6L as the parton distribution function [59] and set the renormalization scale  $\mu_R$  and factorization scale  $\mu_F$  to be  $\mu_R = \mu_F = (m_T)/2$ . The SM input parameters are taken as follows [60]:

$$\begin{aligned} m_H &= 125 \text{ GeV}, & m_t &= 173.21 \text{ GeV}, \\ m_W &= 80.385 \text{ GeV}, & \alpha(m_Z) &= 1/127.9, \\ \alpha_s(m_Z) &= 0.1185, & G_F &= 1.166370 \times 10^{-5} \text{ GeV}^{-2}. \end{aligned} \quad (3)$$

In Fig. 2, we show the dependence of the cross sections  $\sigma$  for the process  $pp \rightarrow Tj + \bar{T}j$  on the  $T$  quark mass  $m_T$  at

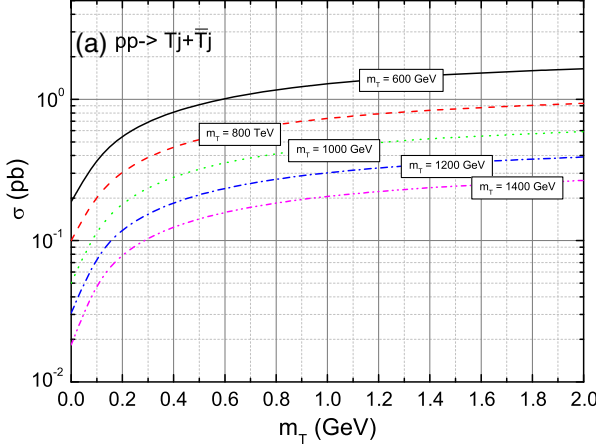


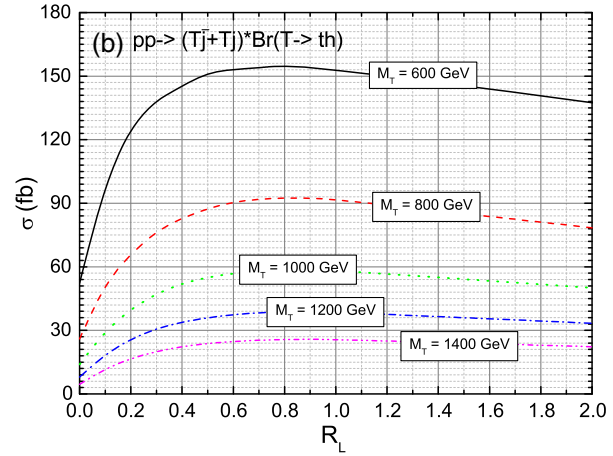
FIG. 3. The dependence of the cross sections  $\sigma$  on the mixing parameter  $R_L$  at 14 TeV LHC for the processes (a)  $pp \rightarrow (Tj + \bar{T}j)$  and (b)  $pp \rightarrow (Tj + \bar{T}j) \rightarrow (t + \bar{t})hj$ . Here we take  $g^* = 0.1$  and five typical  $T$  quark masses  $m_H = 600, 800, 1000, 1200$  and  $1400$  GeV, respectively.

the 14 TeV LHC for  $g^* = 0.1$  and several values of  $R_L$ . For comparison, we also show the  $T\bar{T}$  pair production cross section. One can see that, even without mixing (in the case of  $R_L = 0$ ), the single production of top partners starts to dominate over pair production for  $m_T \gtrsim 1$  TeV. On the other hand, the values of the single production cross sections are very sensitive to  $R_L$ . This implies that the mixing with the first generation can enhance the single production, especially due to the presence of valence quarks in the initial state.

In Figs. 3(a) and 3(b), we show the dependence of the cross sections  $\sigma$  on the mixing parameter  $R_L$  at the 14 TeV LHC for the processes  $pp \rightarrow (Tj + \bar{T}j)$  and  $pp \rightarrow (Tj + \bar{T}j) \rightarrow (t + \bar{t})hj$ , respectively. We generate five benchmark points, varying the  $T$  quark mass in steps of 200 GeV in the range [600; 1400] GeV with  $g^* = 0.1$ . One can see that (i) in the range of  $R_L < 1$ , the production cross sections for the processes  $pp \rightarrow (Tj + \bar{T}j)$  and  $pp \rightarrow (Tj + \bar{T}j) \rightarrow (t + \bar{t})hj$  both increase largely with the increase of  $R_L$ . (ii) For  $R_L > 1$ , the production cross section for the process  $pp \rightarrow (Tj + \bar{T}j)$  will become slightly large with the increase of  $R_L$ , while the production cross section for the process  $pp \rightarrow (Tj + \bar{T}j) \rightarrow (t + \bar{t})hj$  will become small with the increase of  $R_L$ . This effect is mainly due to the increased admixture of valence quarks in production, mitigated by a reduced  $T \rightarrow th$  branching ratio with increasing  $R_L$ . For the process  $pp \rightarrow (Tj + \bar{T}j) \rightarrow (t + \bar{t})hj$ , the cross section will reach a maximum for  $R_L \simeq 1$ , which corresponds to 50%-50% mixing.

### III. LHC OBSERVABILITY OF $T(\rightarrow th)j \rightarrow t(\rightarrow b\ell^+\nu_\ell)h(\rightarrow \gamma\gamma)j$

In this section, we perform the Monte Carlo simulation and explore the sensitivity of a single top partner at 14 TeV LHC through the channel,



$$pp \rightarrow T(\rightarrow th)j \rightarrow t(\rightarrow b\ell\nu_\ell)h(\rightarrow \gamma\gamma)j. \quad (4)$$

The corresponding free parameters are the top partner mass  $m_T$ , the coupling  $g^*$  which governs the top partner single production, and the mixing parameter  $R_L$ . We take three typical values of the  $T$  quark mass:  $m_T = 600, 800, 1000$  GeV with  $g^* = 0.1$  and  $R_L = 0.5$ . Throughout this analysis, we assume that the presence of a  $T$  quark in the  $h \rightarrow \gamma\gamma$  loop would not change the SM branching ratio value of 0.23%. Obviously, the cross sections are proportional to  $(g^*)^2$ . The QCD next-to-leading order (NLO) prediction for single production is calculated in Refs. [35,61]. Following Ref. [35], here we take the conservative value of the  $K$ -factor as 1.14 for the signal.

Signal and background events are generated at leading order using MadGraph5-aMC@NLO. PYTHIA [62] and Delphes [63] are used to perform the parton shower and the fast detector simulations, respectively. When generating the parton-level events, we assume  $\mu_R = \mu_F$  to be the default event-by-event value. The anti- $k_t$  algorithm [64] with parameter  $\Delta R = 0.4$  is used to reconstruct jets. Lastly, the program of MadAnalysis5 [65] is used for analysis, where the (mis)tagging efficiencies and fake rates are assumed to be their default values.

The main SM backgrounds which yield final states identical to the signal include two parts: the resonant and the nonresonant backgrounds. For the former, they mainly come from the processes that have a Higgs boson decaying to a diphoton in the final states, such as  $thj$  and  $t\bar{t}h$  productions. For the latter, the main background processes contain the diphoton events produced in association with the top quarks, such as  $tj\gamma\gamma$  and  $t\bar{t}\gamma\gamma$  production. Besides, with fake photons due to misidentified jets or electrons, the reducible backgrounds such as  $tj\gamma\gamma$ ,  $t\bar{t}\gamma$  and  $t\bar{t}\gamma j$  can also be the sources of backgrounds for our signal. However, we have not included all these potentially dangerous contributions in the analysis due to very low efficiency (at the order of  $10^{-7}$ ) after applying the suitable cuts. The MLM matching scheme is used,

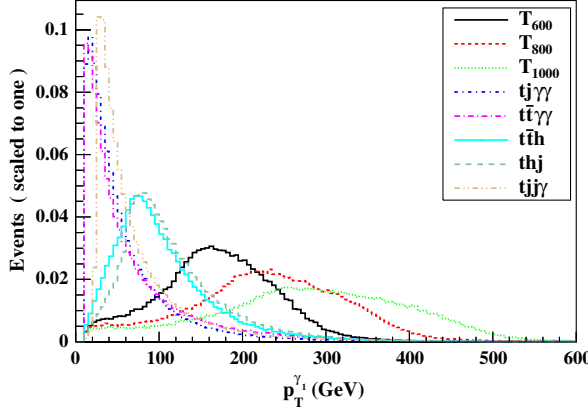


FIG. 4. Normalized distributions of transverse momenta  $p_T^{\gamma_1}$  and  $p_T^{\gamma_2}$  in the signals and backgrounds at 14 TeV LHC.

allowing up to four additional partons in the matrix element [66]. The cross sections of  $thj$  and  $t\bar{t}h$  production are normalized to their NLO values [67,68].

In our simulation, we generate  $10^6$  events for the signals and the backgrounds, respectively. All events are first subject to basic cuts:

- (i) The isolated lepton with transverse momentum  $p_T^\ell > 20$  GeV and  $|\eta_\ell| < 2.5$ .
- (ii) The  $b$ -tagged jet with transverse momentum  $p_T^b > 25$  GeV and  $|\eta_b| < 2.5$ .
- (iii) The light jets with  $p_T^l > 25$  GeV and  $|\eta_l| < 5$ .
- (iv) The photons with  $p_T^\gamma > 20$  GeV and  $|\eta_\gamma| < 2.5$ .

For the signal, we require exactly one charged lepton, one light jet, one  $b$ -jet and two photons in the final state. To trigger the signal events,  $N(\ell) = 1$ ,  $N(b) = 1$  and  $N(j) \leq 2$  are applied, which can help suppress the background events effectively, especially to the events with fake particles.

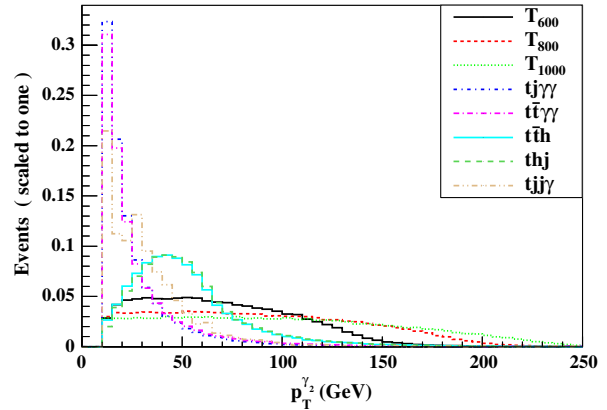
In Figs. 4 and 5, we show the transverse momentum distributions of two photons ( $p_T^{\gamma_1}, p_T^{\gamma_2}$ ) and the invariant mass distribution  $M_{\gamma\gamma}$  in the signal and backgrounds at 14 TeV LHC. Since the two photons in the signal and the resonant backgrounds come from the Higgs boson, they have a harder  $p_T$  spectrum than those in the nonresonant backgrounds. Thus, we can apply the following cuts to suppress the nonresonant backgrounds:

$$p_T^{\gamma_1} > 120 \text{ GeV}, \quad p_T^{\gamma_2} > 60 \text{ GeV}. \quad (5)$$

From Fig. 5, we can see that the signals and the resonant backgrounds, including the Higgs boson, have peaks around 125 GeV. Thus, we can further reduce the nonresonant backgrounds by the following cut:

$$120 \text{ GeV} < M_{\gamma_1\gamma_2} < 130 \text{ GeV}. \quad (6)$$

As defined in MadAnalysis5 [69], the  $T$  quark transverse cluster mass can be reconstructed as



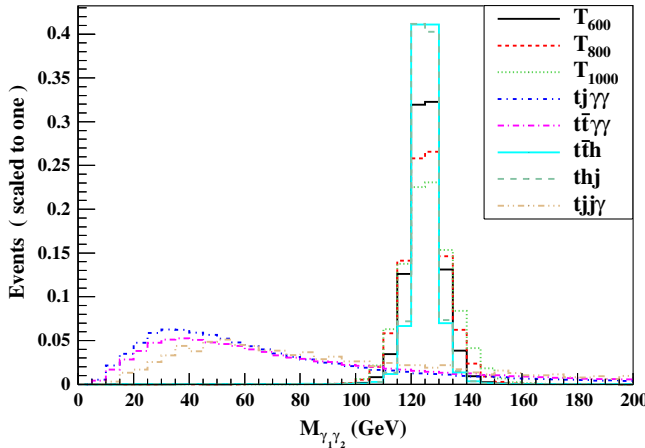


FIG. 5. Normalized invariant mass distribution of two photons at 14 TeV LHC.

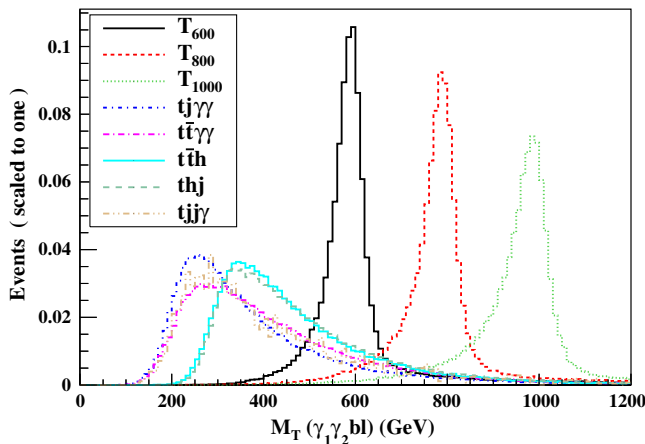


FIG. 6. Normalized transverse mass distribution for the  $\gamma_1\gamma_2 b\ell E_T$  system at 14 TeV LHC.

$$M_T^2 \equiv \left( \sqrt{\left( \sum_{i=\ell,b,\gamma_1,\gamma_2} p_i^2 + \left| \sum_{i=\ell,b,\gamma_1,\gamma_2} \vec{p}_{T,i} \right|^2 \right)^2 - \left| \sum_{i=\ell,b,\gamma_1,\gamma_2} \vec{p}_{T,i} + \vec{p}_T \right|^2} \right)^2 \quad (7)$$

where  $\vec{p}_{T,\ell}$ ,  $\vec{p}_{T,b}$  and  $\vec{p}_{T,\gamma}$  are the transverse momenta of the charged leptons,  $b$ -quarks and photons, respectively,

TABLE I. The cut flow of the cross sections (in  $10^{-3}$  fb) for the signal and backgrounds ( $tj\gamma\gamma$ ,  $t\bar{t}\gamma\gamma$ ,  $t\bar{t}h$ ,  $thj$  and  $tjj\gamma$ ) at the 14 TeV LHC. Here we take the parameters  $g^* = 0.1$  and  $R_L = 0.5$ .

Cuts	Signal for $T_j$							
	600 GeV	800 GeV	1000 GeV	$t\bar{t}h$	$thj$	$tj\gamma\gamma$	$t\bar{t}\gamma\gamma$	$tjj\gamma$
Basic cuts	25.9	15.4	9.57	37.8	4.2	396	184	$21.5 \times 10^3$
Cut 1	6.84	3.92	2.24	0.54	0.08	236	4.6	$2.3 \times 10^3$
Cut 2	3.15	2.38	1.47	0.067	0.075	4.13	0.15	0.63
Cut 3	1.73	1.07	0.59	0.038	0.042	0.074	0.003	0.008
Cut 4	1.69	1.07	0.59	0.015	0.012	0.01	0.001	0.002

and  $\vec{p}_T$  is the missing transverse momentum determined by the negative sum of visible momenta in the transverse direction. In Fig. 6, we show the transverse mass distribution for the  $\gamma_1\gamma_2 b\ell E_T$  system. From this figure, we can see that the transverse mass distribution  $M_T$  has an endpoint around the mass of the top partner. Therefore, we can choose  $M_T > 500$  GeV to reduce the backgrounds.

For a short summary, we require the events to satisfy the following criteria:

- (1) Basic cut:  $p_T^{j,b} > 25$  GeV,  $p_T^{\ell,\gamma} > 20$  GeV,  $|\eta_{b,\ell,\gamma}| < 2.5$ , and  $|\eta_j| < 5$ .
- (2) Cut 1: the basic cuts plus  $N(\ell) = 1$ ,  $N(b) = 1$  and  $N(j) \leq 2$ .
- (3) Cut 2: cut 1 plus exactly two photons [ $N(\gamma) = 2$ ] with  $p_T^{\gamma_1} > 120$  GeV,  $p_T^{\gamma_2} > 60$  GeV.
- (4) Cut 3: cut 2 plus the invariant mass of the diphoton pair to be in the range  $m_h \pm 5$  GeV.
- (5) Cut 4: cut 3 plus  $M_T > 500$  GeV.

The cross sections of the signal and backgrounds after imposing the cuts are summarized in Table I. From Table I, one can see that the jet multiplicity selection  $N(j) \leq 2$  (i.e., cut 1) can efficiently suppress the backgrounds involving  $t\bar{t}$ . By the requirement of exactly two high  $p_T$  photons (i.e., cut 2), all the backgrounds are greatly removed since the photons in the signal are from the boosted Higgs boson in the heavy  $T$  quark decay. Obviously, the nonresonant backgrounds are efficiently reduced by  $\mathcal{O}(10^{-2})$  due to the Higgs mass cut (i.e., cut 3). Thus, all the backgrounds are suppressed very efficiently after imposing all the selections.

To estimate the observability quantitatively, we adopt the significance measurement [70]

$$SS = \sqrt{2L \left[ (S+B) \ln \left( 1 + \frac{S}{B} \right) - S \right]}, \quad (8)$$

where  $S$  and  $B$  are the signal and background cross sections and  $L$  is the integrated luminosity. Here we define the discovery significance as  $SS = 5$  and exclusion limits as  $SS = 3$ . From Table I, we see that the cross sections for the signal are only at the level of  $10^{-3}$  fb, and thus we take a high integrated luminosity of  $3 \text{ ab}^{-1}$  at the 14 TeV LHC. The cross section for an arbitrary value of  $R_L$  is calculated

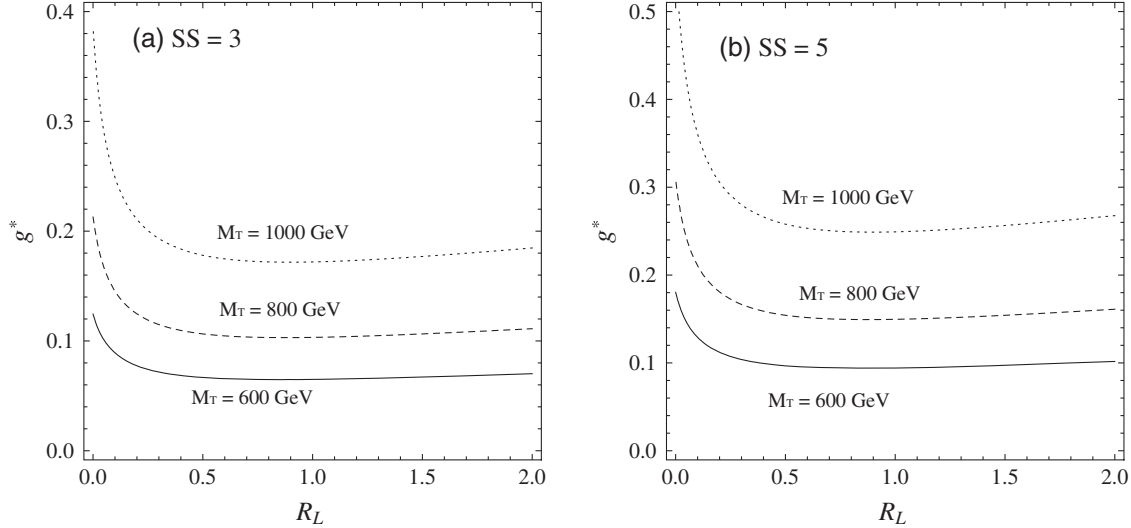


FIG. 7. The  $3\sigma$  (left) and  $5\sigma$  (right) contour plots for the signal in  $g^* - R_L$  at 14 TeV LHC with  $3 \text{ ab}^{-1}$  of integrated luminosity.

following the method in Ref. [46], which has been presented in the Appendix.

In Fig. 7, we plot the excluded  $3\sigma$  and  $5\sigma$  discovery reaches in the plane of  $g^* - R_L$  for three fixed typical  $T$  masses at 14 TeV LHC with  $3 \text{ ab}^{-1}$  of integrated luminosity. From Fig. 7, one can see that the  $5\sigma$  level discovery sensitivity of  $g^*$  is about 0.18 (0.31) for  $m_T = 600(800)$  GeV and  $R_L = 0$ , and it changes as 0.1(0.16) for the nonvanishing  $R_L$ . As mentioned before, the cross section for the final state (and hence the LHC) reaches a maximum for  $R_L \approx 1$  due to the mixing effects. On the other hand, from the  $3\sigma$  exclusion limits one can see that the upper limits on the size of  $g^*$  are given as  $g^* \leq 0.12(0.21)$  for  $m_T = 600(800)$  GeV and  $R_L = 0$  and that they change as  $g^* \leq 0.08(0.11)$  for the nonvanishing  $R_L$ .

#### IV. CONCLUSION

The new heavy vectorlike top partner of charge 2/3 appears in many new physics models beyond the SM. In this paper, we exploited a simplified model with only three free parameters: the top partner mass  $m_T$ , the electroweak coupling constant  $g^*$  and the generation mixing parameter  $R_L$ . We first calculated the cross section for the single  $T$  production with the decay channel  $T \rightarrow th$ . Then, we investigated the observability of the heavy vectorlike top partner  $T$  production through the process  $pp \rightarrow T(\rightarrow th)j \rightarrow t(\rightarrow b\ell\nu_\ell)h(\rightarrow \gamma\gamma)j$  at the HL-LHC. The  $3\sigma$  exclusion limits, as well as the  $5\sigma$  discovery reach in the parameter plane of the two variables  $g^* - R_L$ , are obtained for three typical heavy  $T$  quark masses  $m_T = 600$ , 800 and 1000 GeV, respectively. For  $m_T = 600(800)$  GeV, the upper limits on the size of  $g^*$  are given as  $g^* \leq 0.12(0.21)$  for  $R_L = 0$  and  $g^* \leq 0.08(0.11)$  for the nonvanishing  $R_L$ .

#### ACKNOWLEDGMENTS

This work is supported by the Joint Funds of the National Natural Science Foundation of China (U1304112) and the Foundation of Henan Educational Committee (2015GGJS-059).

#### APPENDIX: CROSS SECTION FOR AN ARBITRARY VALUE OF $R_L$

Following the method in Ref. [46], the cross section for an arbitrary value of  $R_L$  is given by<sup>2</sup>

$$\sigma(m_T, R_L) = \sigma(m_T, 0.5) \times \frac{\sigma_{pp \rightarrow Tj}(m_T, R_L) \text{Br}_{T \rightarrow th}(m_T, R_L)}{\sigma_{pp \rightarrow Tj}(m_T, 0.5) \text{Br}_{T \rightarrow th}(m_T, 0.5)} \quad (A1)$$

where

$$\begin{aligned} \sigma_{pp \rightarrow Tj}(m_T, R_L) &= \frac{R_L}{1 + R_L} \mathcal{A}_{R_L \rightarrow \infty}(m_T) \\ &\quad + \frac{1}{1 + R_L} \mathcal{A}_{R_L=0}(m_T), \end{aligned} \quad (A2)$$

$$\text{Br}_{T \rightarrow th}(m_T, R_L) = \frac{1}{1 + R_L} \mathcal{B}(m_T). \quad (A3)$$

Here  $\mathcal{A}_{R_L \rightarrow \infty}$  and  $\mathcal{A}_{R_L=0}$ , respectively, represent the production cross section for the heavy  $T$  quark due to the interaction to partons belonging to the first and third generations. Note that  $\mathcal{B}(m_T)$  is the  $T$  quark branching

<sup>2</sup>For a more detailed interpretation of this method, see Sec. II.1 in Ref. [46]. Here we also consider the case in which the  $T$  decay products are much lighter than its mass.

ratio for its decay into a top quark and a SM Higgs boson, which can be calculated automatically by using MadGraph5-aMC@NLO.

Obviously, such a cross section also depends on the choice of the PDF and the EW couplings, etc. By

considering the ratio of the cross sections evaluated at different values of  $R_L$ , one can factorize the impact of the above choices. Thus, such a ratio can be used to rescale a given cross section, evaluated by the choice of  $R_L$ .

- 
- [1] G. Aad *et al.* (ATLAS Collaboration), *Phys. Lett. B* **716**, 1 (2012).
- [2] S. Chatrchyan *et al.* (CMS Collaboration), *Phys. Lett. B* **716**, 30 (2012).
- [3] P. H. Frampton, P. Q. Hung, and M. Sher, *Phys. Rep.* **330**, 263 (2000).
- [4] A. De Simone, O. Matsedonskyi, R. Rattazzi, and A. Wulzer, *J. High Energy Phys.* **04** (2013) 004.
- [5] N. Arkani-Hamed, A. G. Cohen, E. Katz, and A. E. Nelson, *J. High Energy Phys.* **07** (2002) 034; N. Arkani-Hamed, A. G. Cohen, E. Katz, A. E. Nelson, T. Gregoire, and J. G. Wacker, *J. High Energy Phys.* **08** (2002) 021; M. Schmaltz and D. Tucker-Smith, *Annu. Rev. Nucl. Part. Sci.* **55**, 229 (2005).
- [6] I. Antoniadis, *Phys. Lett. B* **246**, 377 (1990); D. B. Kaplan, *Nucl. Phys.* **B365**, 259 (1991); K. Agashe, G. Perez, and A. Soni, *Phys. Rev. D* **75**, 015002 (2007).
- [7] K. Agashe, R. Contino, and A. Pomarol, *Nucl. Phys.* **B719**, 165 (2005).
- [8] Z. Chacko, H.-S. Goh, and R. Harnik, *Phys. Rev. Lett.* **96**, 231802 (2006); Z. Chacko, Y. Nomura, M. Papucci, and G. Perez, *J. High Energy Phys.* **01** (2006) 126.
- [9] L. Lavoura and J. P. Silva, *Phys. Rev. D* **47**, 2046 (1993); C. Balazs, H.-J. He, and C.-P. Yuan, *Phys. Rev. D* **60**, 114001 (1999); H.-J. He, N. Polonsky, and S. Su, *Phys. Rev. D* **64**, 053004 (2001); J. A. Aguilar-Saavedra, *Phys. Lett. B* **625**, 234 (2005); G. Cynolter and E. Lendvai, *Eur. Phys. J. C* **58**, 463 (2008); J. A. Aguilar-Saavedra, *J. High Energy Phys.* **11** (2009) 030.
- [10] P. Meade and M. Reece, *Phys. Rev. D* **74**, 015010 (2006); R. Contino and G. Servant, *J. High Energy Phys.* **06** (2008) 026; M. M. Nojiri and M. Takeuchi, *J. High Energy Phys.* **10** (2008) 025; J. Alwall, J. L. Feng, J. Kumar, and S. Su, *Phys. Rev. D* **81**, 114027 (2010); G. Cacciapaglia, A. Deandrea, D. Harada, and Y. Okada, *J. High Energy Phys.* **11** (2010) 159; J. Berger, J. Hubisz, and M. Perelstein, *J. High Energy Phys.* **07** (2012) 016; Y. Okada and L. Panizzi, *Adv. High Energy Phys.* **2013**, 364936 (2013); X.-F. Wang, C. Du, and H.-J. He, *Phys. Lett. B* **723**, 314 (2013).
- [11] H.-C. Cheng, I. Low, and L.-T. Wang, *Phys. Rev. D* **74**, 055001 (2006); S. Matsumoto, M. M. Nojiri, and D. Nomura, *Phys. Rev. D* **75**, 055006 (2007); Y.-B. Liu, X.-L. Wang, and Y.-H. Cao, *Chin. Phys. Lett.* **24**, 57 (2007); C.-X. Yue, L.-H. Wang, and J. Wang, *Chin. Phys. Lett.* **25**, 1613 (2008); Q.-H. Cao, C. S. Li, and C.-P. Yuan, *Phys. Lett. B* **668**, 24 (2008); C.-X. Yue, H.-D. Yang, and W. Ma, *Nucl. Phys.* **B818**, 1 (2009); C.-X. Yue, X.-S. Su, W. Ma, and T.-T. Zhang, *Chin. Phys. Lett.* **27**, 101203 (2010).
- [12] C.-Y. Chen, A. Freitas, T. Han, and K. S. M. Lee, *J. High Energy Phys.* **11** (2012) 124; J. Kearney, A. Pierce, and J. Thaler, *J. High Energy Phys.* **10** (2013) 230; G. Burdman, Z. Chacko, R. Harnik, L. de Lima, and C. B. Verhaaren, *Phys. Rev. D* **91**, 055007 (2015); A. Anandakrishnan, J. H. Collins, M. Farina, E. Kuflik, and M. Perelstein, *Phys. Rev. D* **93**, 075009 (2016).
- [13] G. Dissertori, E. Furlan, F. Moortgat, and P. Nef, *J. High Energy Phys.* **09** (2010) 019; N. Chen and H.-J. He, *J. High Energy Phys.* **04** (2012) 062; O. Matsedonskyi, G. Panico, and A. Wulzer, *J. High Energy Phys.* **01** (2013) 164; T. Flacke, J. H. Kim, S. J. Lee, and S. H. Lim, *J. High Energy Phys.* **05** (2014) 123; B. Gripaios, T. Mueller, M. A. Parker, and D. Sutherland, *J. High Energy Phys.* **08** (2014) 171.
- [14] J. Serra, *J. High Energy Phys.* **09** (2015) 176; T. DeGrand and Y. Shamir, *Phys. Rev. D* **92**, 075039 (2015); O. Matsedonskyi, G. Panico, and A. Wulzer, *J. High Energy Phys.* **04** (2016) 003.
- [15] H.-S. Goh and C. A. Krenke, *Phys. Rev. D* **81**, 055008 (2010); Y.-B. Liu and X.-L. Wang, *Int. J. Mod. Phys. A* **25**, 5885 (2010); Y.-B. Liu and Z.-J. Xiao, *Nucl. Phys.* **B892**, 63 (2015); H.-C. Cheng, S. Jung, E. Salvioni, and Y. Tsai, *J. High Energy Phys.* **03** (2016) 074.
- [16] C.-H. Chen and T. Nomura, *Phys. Rev. D* **94**, 035001 (2016); S. Moretti, D. O'Brien, L. Panizzi, and H. Prager, arXiv:1603.09237; M. Endo and Y. Takaesu, *Phys. Lett. B* **758**, 355 (2016).
- [17] E. L. Berger and Q.-H. Cao, *Phys. Rev. D* **81**, 035006 (2010); B. Holdom and Q.-S. Yan, *Phys. Rev. D* **83**, 114031 (2011); **84**, 094012 (2011); S. Yang, J. Jiang, Q.-S. Yan, and X. Zhao, *J. High Energy Phys.* **09** (2014) 035.
- [18] S. Gopalakrishna, T. Mandal, S. Mitra, and G. Moreau, *J. High Energy Phys.* **08** (2014) 079; C. Han, A. Kobakhidze, N. Liu, L. Wu, and B. Yang, *Nucl. Phys.* **B890**, 388 (2014); S. A. R. Ellis, R. M. Godbole, S. Gopalakrishna, and J. D. Wells, *J. High Energy Phys.* **09** (2014) 130; M. Endo, K. Hamaguchi, K. Ishikawa, and M. Stoll, *Phys. Rev. D* **90**, 055027 (2014); S. Beauceron, G. Cacciapaglia, A. Deandrea, and J. D. Ruiz-Alvarez, *Phys. Rev. D* **90**, 115008 (2014).
- [19] N. Arkani-Hamed, T. Han, M. Mangano, and L.-T. Wang, *Phys. Rep.* **652**, 1 (2016); G. Brooijmans *et al.*, arXiv: 1405.1617; arXiv:1605.02684; M. Buchkremer, arXiv: 1405.2586.
- [20] ATLAS Collaboration, Report No. ATLAS-CONF-2013-018, 2013; Report No. ATLAS-CONF-2014-036, 2014; Report No. ATLAS-CONF-2013-060, 2013; *J. High Energy Phys.* **11** (2014) 104; *J. High Energy Phys.* **10** (2015) 150;

- J. High Energy Phys. 08 (2015) 105; Report No. ATLAS-CONF-2016-013, 2016.
- [21] CMS Collaboration, Report No. CMS-PAS-JME-13-007, 2014; Phys. Lett. B **729**, 149 (2014); Phys. Rev. D **93**, 012003 (2016); Report No. CMS-PAS-B2G-16-002, 2016.
- [22] M. E. Peskin and T. Takeuchi, Phys. Rev. D **46**, 381 (1992); G. Altarelli and R. Barbieri, Phys. Lett. B **253**, 161 (1991).
- [23] J. Hubisz and P. Meade, Phys. Rev. D **71**, 035016 (2005); H.-J. He, T. M. P. Tait, and C.-P. Yuan, Phys. Rev. D **62**, 011702 (2000); J. Hubisz, P. Meade, A. Noble, and M. Perelstein, J. High Energy Phys. 01 (2006) 135.
- [24] A. Djouadi, J. H. Kuhn, and P. M. Zerwas, Z. Phys. C **46**, 411 (1990); F. Boudjema, A. Djouadi, and C. Verzegnassi, Phys. Lett. B **238**, 423 (1990); R. S. Chivukula, B. Coleppa, S. D. Chiara, E. H. Simmons, H.-J. He, M. Kurachi, and M. Tanabashi, Phys. Rev. D **74**, 075011 (2006); E. L. Berger, Q.-H. Cao, and I. Low, Phys. Rev. D **80**, 074020 (2009).
- [25] J. A. Aguilar-Saavedra, R. Benbrik, S. Heinemeyer, and M. Perez-Victoria, Phys. Rev. D **88**, 094010 (2013).
- [26] V. Khachatryan *et al.* (CMS Collaboration), Eur. Phys. J. C **75**, 212 (2015); G. Aad *et al.* (ATLAS Collaboration), Eur. Phys. J. C **76**, 6 (2016); ATLAS and CMS Collaborations, Report No. ATLAS-CONF-2015-044.
- [27] A. Atre, M. Chala, and J. Santiago, J. High Energy Phys. 05 (2013) 099; A. Djouadi, Eur. Phys. J. C **73**, 2498 (2013); C.-Y. Chen, S. Dawson, and I. M. Lewis, Phys. Rev. D **90**, 035016 (2014); A. Djouadi, J. Quevillon, and R. Vega-Morales, Phys. Lett. B **757**, 412 (2016); S. Dittmaier *et al.* (LHC Higgs Cross Section Working Group Collaboration), arXiv:1101.0593.
- [28] X.-F. Wang, C. Du, and H.-J. He, Phys. Lett. B **723**, 314 (2013); T. Abe, M. Chen, and H.-J. He, J. High Energy Phys. 01 (2013) 082; J. Baglio and A. Djouadi, J. High Energy Phys. 03 (2011) 055; S. Fichet and G. Moreau, Nucl. Phys. **B905**, 391 (2016); A. Angelescu, A. Djouadi, and G. Moreau, Eur. Phys. J. C **76**, 99 (2016).
- [29] A. De Simone, O. Matsedonskyi, R. Rattazzi, and A. Wulzer, J. High Energy Phys. 04 (2013) 004.
- [30] A. Azatov, M. Salvarezza, M. Son, and M. Spannowsky, Phys. Rev. D **89**, 075001 (2014).
- [31] M. Backović, T. Flacke, S. J. Lee, and G. Perez, J. High Energy Phys. 09 (2015) 022; M. Backović, T. Flacke, J. H. Kim, and S. J. Lee, Phys. Rev. D **92**, 011701 (2015).
- [32] N. Vignaroli, J. High Energy Phys. 07 (2012) 158.
- [33] N. Vignaroli, Phys. Rev. D **86**, 075017 (2012).
- [34] N. Gutierrez, J. Ferrando, D. Kar, and M. Spannowsky, Phys. Rev. D **90**, 075009 (2014); S. Beauceron, G. Cacciapaglia, A. Deandrea, and J. D. Ruiz-Alvarez, Phys. Rev. D **90**, 115008 (2014); J. Li, D. Liu, and J. Shu, J. High Energy Phys. 11 (2013) 047.
- [35] J. Reuter and M. Tonini, J. High Energy Phys. 01 (2015) 088.
- [36] M. Backovic, T. Flacke, J. H. Kim, and S. J. Lee, J. High Energy Phys. 04 (2016) 014.
- [37] ATLAS Collaboration, J. High Energy Phys. 02 (2016) 110; Eur. Phys. J. C **76**, 442 (2016); Phys. Lett. B **758**, 249 (2016); Report No. ATLAS-CONF-2016-072, 2016.
- [38] CMS Collaboration, Report No. CMS-PAS-B2G-15-008, 2016.
- [39] G. Cacciapaglia, A. Deandrea, D. Harada, and Y. Okada, J. High Energy Phys. 11 (2010) 159.
- [40] F. del Aguila, M. Perez-Victoria, and J. Santiago, J. High Energy Phys. 09 (2000) 011; G. Cacciapaglia, A. Deandrea, L. Panizzi, N. Gaur, D. Harada, and Y. Okada, J. High Energy Phys. 03 (2012) 070; F. J. Botella, G. C. Branco, and M. Nebot, J. High Energy Phys. 12 (2012) 040.
- [41] K. Ishiwata, Z. Ligeti, and M. B. Wise, J. High Energy Phys. 10 (2015) 027; A. K. Alok, S. Banerjee, D. Kumar, S. U. Sankar, and D. London, Phys. Rev. D **92**, 013002 (2015); F. J. Botella, G. C. Branco, M. Nebot, M. N. Rebelo, and J. I. Silva-Marcos, arXiv:1610.03018.
- [42] M. Buchkremer, G. Cacciapaglia, A. Deandrea, and L. Panizzi, Nucl. Phys. **B876**, 376 (2013).
- [43] S. A. R. Ellis, R. M. Godbole, S. Gopalakrishna, and J. D. Wells, J. High Energy Phys. 09 (2014) 130.
- [44] G. Cacciapaglia, A. Deandrea, N. Gaur, D. Harada, Y. Okada, and L. Panizzi, J. High Energy Phys. 09 (2015) 012.
- [45] A. Atre, G. Azuelos, M. Carena, T. Han, E. Ozcan, J. Santiago, and G. Unel, J. High Energy Phys. 08 (2011) 080.
- [46] L. Basso and J. Andrea, J. High Energy Phys. 02 (2015) 032.
- [47] C. Grojean, O. Matsedonskyi, and G. Panico, J. High Energy Phys. 10 (2013) 160.
- [48] D. Barducci, A. Belyaev, J. Blamey, S. Moretti, L. Panizzi, and H. Prager, J. High Energy Phys. 07 (2014) 142.
- [49] D. Barducci, A. Belyaev, M. Buchkremer, G. Cacciapaglia, A. Deandrea, S. De Curtis, J. Marrouche, S. Moretti, and L. Panizzi, J. High Energy Phys. 12 (2014) 080.
- [50] O. Matsedonskyi, G. Panico, and A. Wulzer, J. High Energy Phys. 12 (2014) 097.
- [51] D. Pappadopulo, A. Thamm, R. Torre, and A. Wulzer, J. High Energy Phys. 09 (2014) 060.
- [52] N. Liu, L. Wu, B.-F. Yang, and M.-C. Zhang, Phys. Lett. B **753**, 664 (2016).
- [53] Y.-B. Liu and Z.-J. Xiao, Phys. Rev. D **94**, 054018 (2016); Phys. Lett. B **763**, 458 (2016).
- [54] CMS Collaboration, Report No. CMS-PAS-B2G-14-003, 2014.
- [55] See [https://feynrules.irmp.ucl.ac.be/wiki/VLQ\\_tsingletlv](https://feynrules.irmp.ucl.ac.be/wiki/VLQ_tsingletlv).
- [56] A. Alloul, N. D. Christensen, C. Degrande, C. Duhr, and B. Fuks, Comput. Phys. Commun. **185**, 2250 (2014).
- [57] J. Alwall, R. Frederix, S. Frixione, V. Hirschi, F. Maltoni, O. Mattelaer, H.-S. Shao, T. Stelzer, P. Torrielli, and M. Zaro, J. High Energy Phys. 07 (2014) 079.
- [58] A. Belyaev, N. D. Christensen, and A. Pukhov, Comput. Phys. Commun. **184**, 1729 (2013).
- [59] J. Pumplin, A. Belyaev, J. Huston, D. Stump, and W. K. Tung, J. High Energy Phys. 02 (2006) 032.
- [60] K. A. Olive *et al.* (Particle Data Group Collaboration), Chin. Phys. C **38**, 090001 (2014).
- [61] B. Fuks and H.-S. Shao, arXiv:1610.04622.
- [62] T. Sjostrand, S. Mrenna, and P. Z. Skands, J. High Energy Phys. 05 (2006) 026.
- [63] J. de Favereau, C. Delaere, P. Demin, A. Giannanco, V. Lemaître, A. Mertens, and M. Selvaggi (DELPHES 3 Collaboration), J. High Energy Phys. 02 (2014) 057.
- [64] M. Cacciari, G. P. Salam, and G. Soyez, J. High Energy Phys. 04 (2008) 063.

- [65] E. Conte, B. Fuks, and G. Serret, *Comput. Phys. Commun.* **184**, 222 (2013).
- [66] M. L. Mangano, M. Moretti, F. Piccinini, and M. Treccani, *J. High Energy Phys.* 01 (2007) 013; R. Frederix and S. Frixione, *J. High Energy Phys.* 12 (2012) 061.
- [67] M. Farina, C. Grojean, F. Maltoni, E. Salvioni, and A. Thamm, *J. High Energy Phys.* 05 (2013) 022.
- [68] S. Frixione, V. Hirschi, D. Pagani, H.-S. Shao, and M. Zaro, *J. High Energy Phys.* 06 (2015) 184; Y. Zhang, W. G. Ma, R. Y. Zhang, C. Chen, and L. Guo, *Phys. Lett. B* **738**, 1 (2014).
- [69] E. Conte, B. Dumont, B. Fuks, and C. Wymant, *Eur. Phys. J. C* **74**, 3103 (2014).
- [70] G. Cowan, K. Cranmer, E. Gross, and O. Vitells, *Eur. Phys. J. C* **71**, 1 (2011).